Autophagy Mitigates High-Temperature Injury during Microsporogenesis in *Arabidopsis thaliana*

Atsushi Higashitani[1*†], Zhenhua Shao[1*], Mami Kikuta, Sakuya Nakamura, Masanori Izumi[1,2*]

[1] Graduate School of Life Sciences, Tohoku University, Sendai 980-8577, Japan

[2] Frontier Research Institute for Interdisciplinary Sciences, Tohoku University, Sendai, 980-8578, Japan

*These authors contributed equally to this work.

†To whom correspondence should be addressed. 2-1-1, Katahira, Aoba-ku, Sendai, Miyagi 980-8577, Japan. Tel: +81-22-217-5715. Fax: +81-22-217-5691. E-mail: ahigashi@m.tohoku.ac.jp

Running title: HT-induced autophagy in microsporogenesis

Abstract

Autophagy degrades cellular components during senescence, starvation, and stress. High-temperature (HT) stress can inhibit microsporogenesis, but the involvement of autophagy in HT injury is unknown. Here we show that Arabidopsis autophagy-defective (*atg*) mutants are hypersensitive to HT stress during microsporogenesis but not during seedling growth. Fertility was normal at 23 °C, but sporophytic male sterility occurred at 30 °C. At 30 °C, wild-type developing anthers showed increased vacuolization in tapetum and lipophagy in microspores. The *atg5-1* mutant did not show these autophagic phenomena, but instead showed irregularly enlarged vacuoles and subsequent shrinkage, and failure of the tapetum to degenerate completely. HT specifically upregulated ATG8 in the developing anther, but not in seedlings, and reduced MYB80 signaling in the anther, which is required for the regulation of tapetal programmed cell death to promote microspore maturation. Interestingly, inhibition of auxin activated the ATG8 signal in seedlings at both 23 and 30 °C. These results, combined with our previous observation of anther-specific auxin depletion caused by HT, suggest that autophagy mitigates HT injury to microsporogenesis by supporting tapetal degeneration and micropore maturation in response to auxin reduction.

Keywords: ATG / Auxin / PCD / Sterility / Tapetum /

Introduction

Autophagy is a catabolic process of degradation of cellular components within lysosomes

in eukaryotes, and is highly conserved from yeasts to plants and mammals (Ohsumi 1999, Klionsky & Emr, 2000; Yorimitsu & Klinosky 2005; 2007; Kim et al. 2007; Nakatogawa et al. 2009; Yoshimoto 2012). In plants, autophagy is active during cell development, nutrient starvation, senescence, and stress due to pathogens, drought, salt, and oxidation (Bassham et al. 2006; Hofius et al. 2011; Yoshimoto 2012). In Arabidopsis and rice, a series of autophagy-related (*ATG*) genes have been identified, as most of the essential residues are well conserved between yeasts and plants (Doelling et al. 2002; Hanaoka et al. 2002; Chung et al. 2009; Xia et al. 2011; Yoshimoto 2012). It also functions in autophagic, or type II, programmed cell death (PCD) through hyperactivation in mammals and plants (Baehrecke 2005; Kroemer & Jäättelä 2005; Love et al. 2008; Parish & Li 2009). Apoptosis or type I PCD is involved in rapid responses, such as the hypersensitivity response to a pathogen, whereas autophagic PCD functions more slowly and thus is represented in leaf senescence (Love et al. 2008; Parish & Li 2009; Wada et al. 2015).

Anther development, including specification of cell lineage and fate, follows well regulated programs. Apoptosis must break down anther wall tapetum cells for pollen grains to mature (Papini et al. 1999; Varnier et al. 2005). Chromatin condensation, DNA fragmentation, and mitochondrial disintegration lead to rapid cell death. In particular, the MYB80 transcription factor is required for the regulation of apoptotic tapetal PCD in Arabidopsis, rice, wheat, and cotton (Phan et al 2011; 2012; Su et al 2014). As Arabidopsis *atg* mutants can complete their life cycles under normal culture conditions, autophagy is dispensable for tapetal PCD and pollen development in general (Yoshimoto 2012). Moreover, a transgenic tobacco line overexpressing Arabidopsis *AtATG6/BECLIN1* in the tapetum cells showed male sterility (Singh et al 2010; 2015). Thus, it seems that autophagy should be harmful to normal microsporogenesis in Arabidopsis. On the other hand, the rice autophagy null mutant *OsATG7* showed a defect in tapetum cell degradation and sporophytic male sterility under normal culture conditions (Kurusu et al. 2014; Hanamata et al. 2014). Hence, the biological significance and function of autophagy during microsporogenesis remain unclear.

Early anther development is highly susceptible to environmental stresses. We previously found that high temperature (HT) caused the premature degradation of tapetum cells and abnormal vacuolization (Abiko et al. 2005; Oshino et al. 2007; 2011). In addition, male sterility in Arabidopsis and barley is caused by HT-promoted depletion of auxin in anthers (Sakata et al. 2010). However, it is not clear whether elevated temperatures directly induce autophagy, and if so, how autophagy is involved in the response of microsporogenesis to HT.

Here we evaluated the sensitivity of Arabidopsis *atg* mutants to HT stress and used histology to compare the degradation of tapetum cells and pollen development between wild-type Col-0 (WT) and *atg* mutants under HT. HT reduced MYB80 signaling and induced the expression of autophagy marker *ATG8* genes in the WT developing anthers. We also clarified the relationship between auxin depletion and autophagy induction in seedlings.

Results

Arabidopsis *atg* mutants are hypersensitive to HT injury and show sporophytic male sterility

To assess the effect of autophagy on the damage caused reproductive development by HT, we measured silique elongation of WT and *atg* mutant plants at 23 and 30 °C. In WT plants moved from 23 °C to 30 °C, silique length was reduced by up to two-thirds from the 5th to the terminal blossoms relative to plants held at 23 °C (Fig. 1). The 5th flower was at floral stage 10-11 (Smyth et al. 1990) when the plants were moved, indicating that this stage is critical for susceptibility to elevated temperatures. In contrast, in all tested *atg* mutants, silique elongation were completely lost from the 5th to the terminal blossoms after plants were moved, whereas fertility was normal at 23 °C (Fig. 1). Over the 7 days after transfer to 30 °C, the siliques withered early in the *atg* mutants (Fig. 2A–G).

When either WT or *atg5-1* pistils (n = 5) that had developed at 30 °C were pollinated with their respective pollen that had developed at 23 °C, but not at 30 °C, their silique elongation were fully rescued, indicating an exclusively male effect (Fig. 2H, I).

At 30 °C, the number of mature pollen grains in the anthers at anthesis (floral stage 13) was reduced by approximately half in WT (Fig. 3J, N), but was reduced almost totally in the *atg5-1* mutant, and those that remained were severely degenerated (Fig. 3L, P). At 23 °C, however, megaspores developed normally in both WT and *atg5-1*. These results indicate that HT at 30 °C caused complete sporophytic male sterility in the *atg* mutant.

Autophagy is induced in tapetum cells and microspores by elevated temperatures

The tapetum (anther wall) cells disappeared completely at floral stage 13 in WT grown at either 23 or 30 °C (Fig. 3M, N). They degraded normally at 23 °C in *atg5-1*, but patches remained at 30 °C (Fig. 3O, P). To further investigate how autophagy mitigates HT injury, we dissected the floral stage 10–11 anthers of WT and *atg5-1* plants grown at 30 °C for 3 days. Transmission electron microscopy showed that uninucleate pollen grains developed in all specimens (Fig. 4). At 23 °C, the tapetosomes and elaioplasts (components of the pollen coat) developed normally in anther tapeta of both WT and *atg5-1* (Fig. 4C, I). At 30 °C in WT, tapetosomes developed abnormal vacuoles and elaioplasts developed larger vacuoles with irregularly fused plastoglobuli (Fig. 4F). In addition, the WT microspores showed lipophagy-like lipid bodies trapped in their vacuoles and gained electron density (Fig. 4E), and other vacuoles captured cytoplasms also increased in microspores and anther wall cells (Fig. 4E, F).

At 23 °C in *atg5-1*, larger vacuoles often appeared in the anther wall cells (Fig. 4G, I). At 30 °C, abnormal vacuoles in the tapetum and microspores were enlarged, and the tapetum showed increased electron density but shrank incompletely (Fig. 4J, L). However, *atg5-1* did not show either vacuolization of elaioplasts and tapetosomes or the lipophagy-like structures of microspores observed in WT in spite of their electron density increased (Fig. 4K, L). These strongly suggest that autophagy would promote degradation of elaioplasts and tapetosomes which leads degeneration of tapetum cells and degrade lipid bodies in microspores, and finally prevents abortion of microspores under elevated temperatures.

To monitor activation of autophagy by HT, we used Arabidopsis YFP-AtATG8e, and RFP-AtATG8i recombinant lines. These recombinant ATG8 proteins are generally used as reliable molecular markers of autophagy in yeast, mammal, and Arabidopsis cells (Mizusima et al. 2004; Xie et al. 2008; Ishida et al. 2008; Nakayama et al. 2012; Merkulova et al. 2014). At 30 °C, the YFP-ATG8e and RFP-ATG8i recombinant lines showed increased fluorescence and larger dots in the anther wall tapetum cells and weakly but significantly in the microspores at floral stage 10-11 (Fig. 5C, G). In addition, real-time RT-PCR analyses confirmed that not only *ATG8e* and *ATG8i* but also *ATG8a* were upregulated in developing (floral stage 10-11) anthers of WT (Fig. 6). These results strongly suggest that the lipophagy-like structures of microspores and the vacuolization of elaioplasts and tapetosomes observed in WT at 30 °C are due to activation of autophagy.

Elevated temperature repressed MYB80 signaling in developing anther cells

MYB80 is required for the regulation of tapetal PCD (Phan et al. 2011; 2012). It upregulates an A1 aspartic protease called UNDEAD, which controls the timing of tapetal PCD in Arabidopsis (Phan et al. 2011), and downregulates a pectin methylesterase gene, *VANGUARD1* (*VGD1*), and a glyoxal oxidase gene, *GLOX1* (Phan et al. 2011). To elucidate whether HT affects MYB80 transcriptional regulation in developing anther cells, we analyzed the expression of *MYB80*, *UNDEAD*, *VGD1*, and *GLOX1* in dissected anthers at floral stage 10–11. At 30 °C, the expression of *MYB80* was reduced by two orders of magnitude, that of *UNDEAD* was halved, and those of *VGD1* and *GLOX1* were increased by one order of magnitude relative to expression at 23 °C (Fig. 7). These results indicate that HT reduces MYB80 signaling in developing anther cells.

Auxin depletion is a potent inducer of autophagy

To assess whether HT at 30 °C induced autophagy in other tissues of Arabidopsis, we monitored fluorescence in seedling roots of the YFP-ATG8e recombinant line grown at 23 or

30 °C for 3 days. The YFP-ATG8e signal did not increase at elevated temperatures (Fig. 8B, D). In addition, real-time RT-PCR analyses confirmed that the expression of not only *ATG8e* but also *ATG8a* and *ATG8i* did not alter in response to HT in seedling roots of WT (Fig. 9). Moreover, HT retarded root growth almost identically between WT and *atg* plants: by about 20% at 30 °C and severely at 35 °C (Fig. 10). At 30 °C, the expression of *HSP70* and *HSP17.4* was barely if at all induced in the developing anthers or in seedling roots (Fig. 11). At 35 °C, in contrast, expression was much greater in the roots (Fig. 11). These results suggest that both autophagy induction and thermal sensitivity in the *atg* mutants of the developing anther cells, unlike the root cells, might not be directly altered by heat stress.

We previously found that at 30 °C, auxin signaling is specifically repressed in developing anther cells but is increased in seedling roots and developing pistils (Sakata et al. 2010). We therefore applied inhibitors of auxin transport (2,3,5-triiodobenzoic acid: Dhonukshe et al. 2008) and biosynthesis (L-kynurenine: He et al. 2011) to seedlings and evaluated their effects on autophagy induction. The YFP-ATG8e signal was upregulated in the root elongation zone 72 h after treatment with each inhibitor (Fig. 8F, H, J, L). In addition, the expression of *ATG8a*, *ATG8e*, and *ATG8i* approximately doubled in roots at both 23 and 30 °C in the presence of both inhibitors (Fig. 9), as in the developing anthers at 30 °C (Fig. 6). These results suggest that autophagy induction in developing anther cells at 30 °C is caused through anther-specific auxin depletion, not directly by heat.

Discussion

We analyzed the role of autophagy in the response of Arabidopsis plants to the effect of elevated temperatures on reproductive development. Plant autophagy is involved not only in senescence, but also in responses to stress due to nutrient starvation, pathogens, drought, salt, and oxidation (Doelling et al. 2002; Hanaoka et al. 2002; Bassham et al. 2006; Chung et al. 2009; Hofius et al. 2011; Yoshimoto 2012). Recently, Zhou et al. (2014) reported that silencing of *ATG*-related genes reduced the tolerance of tomato to 45 °C. However, these reports concern autophagy during vegetative growth, not reproductive development.

A rice autophagy-defective mutant, the OsATG7 *tos-7* insertion line, is male-sterile owing to the inhibition of tapetum-cell degradation (Kurusu et al. 2014; Hanamata et al. 2014). Lipid bodies appear in the vacuoles during the degradation of normal tapetum cells in rice, so autophagy may be involved in the breakdown of the lipid bodies and of lipids transferred from tapetum cells to the microspore surface (Kurusu et al. 2014; Hanamata et al. 2014). The OsATG7 *tos-7* example indicates that autophagy promotes degeneration of tapetum cells and is essential in at least rice microsporogenesis. However, Arabidopsis autophagy-defective mutants completed their life cycle at normal temperature (Yoshimoto 2012; Figs. 1, 2), and thus rice and Arabidopsis differ in their need for autophagy (Kurusu et al. 2014; Hanamata et al. 2014). In brassicaceous species, including Arabidopsis, a distinctive organelle, the tapetosome, develops in the tapetum cells from the endoplasmic reticulum and stores triacylglycerols, flavonoids, alkanes, and pollen coat proteins (Wu et al. 1997; Suzuki et al. 2013; Hanamata et al. 2014). Another tapetal organelle, the elaioplast, stores a major component of the pollen coat, steryl esters filled with numerous plastoglobuli (Wu et al. 1997; Suzuki et al. 2013; Hanamata et al. 2014).

Arabidopsis *atg* mutants became completely male-sterile at 30 °C whereas WT Col-0 plants still set some seed (Figs. 1, 2). In contrast, there was no difference in retardation of seedling root growth by HT between WT plants and *atg* mutants (Fig. 10). In the roots, 30 °C was not enough to induce autophagy without suppression of auxin (Figs. 8, 9). These results indicate that autophagy mitigates HT injury to microsporogenesis. Our previous report showed that 30 °C caused auxin depletion in the developing anther cells by decreasing anther-specific auxin biosynthesis, although it increased auxin levels in seedling roots and in other developing floral tissues (Sakata et al. 2010). Three days after treatment with auxin inhibitors, autophagy activation was observed as induction of *ATG8* genes and ATG8 proteins in roots at both 23 and 30 °C (Figs. 8, 9). On the other hand, *HSP70* and *HSP17.4* were barely or not

upregulated at 30 °C in either the developing anther cells or the seedling roots (Fig. 11). These results suggest that auxin depletion due to HT stress induces anther-specific autophagy.

Although HT stress affects the whole plant, microsporogenesis is the most sensitive process (Sakata & Higashitani 2008; Müller & Rieu 2016). HT prematurely degrades tapetum cells with increasing vacuolization and increasing mitochondrial and rough endoplasmic reticulum swelling (Oshino et al. 2007; 2011). Overexpression of the Arabidopsis tapetum-cell-specific autophagy-related ATG6/BECLIN1 in tobacco leads to premature degeneration of the developing tapetum cells (Singh et al. 2010; 2015). This might suggest that disrupting autophagy would prevent the premature degradation of tapetum cells and improve HT tolerance. Instead, our results clearly show that autophagy is essential to mitigating HT injury to microsporogenesis in Arabidopsis.

Anther development and differentiation, including specification of cell lineage and cell fate, are well regulated programs. The epidermis, endothecium, middle layer, and tapetum of anther wall cells are sequentially degraded during pollen maturation and anther dehiscence. This degradation process appears to be controlled by PCD (Papini et al. 1999; Varnier et al. 2005; Parish & Li 2010). MYB80 controls the timing of the tapetal PCD, which is conserved in monocot and dicot species (Pan et al. 2011; 2012; Xu et al. 2014). Arabidopsis MYB80 controls at least 70 genes, upregulating *UNDEAD* (by >10×) and downregulating *VGD1* and *GLOX1* (Phan et al. 2011). Either *myb80* or *undead* mutants resulted in complete male sterility with premature tapetal PCD (Li et al. 2007; Phan et al. 2011). In our results in the WT, *UNDEAD* expression was halved and *VGD1* and *GLOX1* were upregulated tenfold in the floral stage 10-11 anthers at 30 °C (Fig. 7), and silique elongation was one third to half (Fig. 1, 2). These results clearly indicate that HT reduces MYB80 transcriptional regulation. At 30 °C, the *ATG8* genes were transcriptionally upregulated in tapetum cells and microspores (Figs. 5, 6). Autophagic vacuoles increased in cytoplasm, elaioplasts and tapetosomes, and lipophagy of lipid bodies increased in microspores (Fig. 4). In mammalian cells, the breakdown of lipid droplets by lipophagy contributes to energy generation under stress conditions (Dong & Czaja 2011). Remarkably, in the *atg5-1* mutant, autophagy did not appear at 30 °C. Instead, abnormal large vacuolization and subsequent shrinkage (but not complete degeneration) of tapetum cells were observed, and the collapse of microspores resulted in complete male sterility (Figs. 3, 4). Together, these results show that HT stress alters the timing of tapetal PCD through repression of MYB80 transcriptional regulation, and sequentially activated autophagy suppresses the alteration by autophagic PCD, rescuing microspore development under HT conditions.

224

Methods

Plant materials and growth conditions

We grew *Arabidopsis thaliana* ecotype Columbia (Col-0). T-DNA knockout mutants of *atg2-1* [SALK_076727], *atg5-1* [SALK_129B07], *atg7-2* [GK-655B06], and *atg10-1* [SALK_084434] were obtained from the Nottingham Arabidopsis Resource Centre. To observe autophagosome formation, we used GFP-AtATG8a transgenic plants (Nakayama et al. 2012), ATG8e promoter-driven YFP-ATG8e expressing plants (*ATG8e*$_{pro}$*:YFP-ATG8e*) and ATG8i promoter-driven mRFP-ATG8i expressing plants (*ATG8i*$_{pro}$*:mRFP-ATG8i*) were generated as follows. The protein coding region of *ATG8e* (At2g45170) were amplified from Arabidopsis cDNA by reverse transcription (RT)-PCR using the following primer pair: ATG8e-F 5'-CAC CAT GAA TAA AGG AAG CAT C; ATG8e-R 5'-TTA GAT TGA AGA AGC ACC GAA TG, cloned into pENTR/D/TOPO (Invitrogen), and transferred to the pUBN-YFP vector (Grefen et al., 2010) to generate YFP-ATG8e fusion. The DNA fragment containing YFP-ATG8e fusion was amplified using the folowing primer pair: YFP-attB1-F 5'-GGG GAC AAG TTT GTA CAA AAA AGC AGG CTT TAT GGT GAG CAA GGG CGA GGA GCT G and ATG8e-attB2R-R 5'-GGG GAC AGC TTT CTT GTA CAA AGT GGT TAG ATT GAA GAA GCA CCG AAT G, and colned into pDONR221 (Invitrogen). The promoter region of *ATG8e*, which include a 2,607 bp upstream region from the start codon, were amplified from Arabidopsis genomic DNA using the following primer pair: ATG8ePro-attB4-F 5'-GGG GAC AAC TTT GTA TAG AAA AGT TGA TCG CAC GGT CCC AAT ATG; ATG8ePro-attB1R-R 5'-GGG GAC TGC TTT TTT GTA CAA ACT TGC TTT GCT TCT GAG AAT ATA CAC AAT C, cloned into pDONR P4-P1R (Invitrogen). To generate the construct expressing YFP-ATG8e fusion under the control of *ATG8e* promoter, pDONR221 containing *YFP-ATG8e* fusion was transferred into R4pGWB501 destination vector (Nakagawa et al., 2008) with pDONR P4-P1R containing promoter region of *ATG8e*. The protein coding region of *ATG8i* (At3g15580) were amplified using the following primer pair: ATG8i-F 5'-CAC CAT GAA ATC GTT CAA GGA AC; ATG8i-R 5'-TCA ACC AAA GGT TTT CTC ACT G, cloned into pENTR/D/TOPO, and transferred to the pUBN-RFP vector (Grefen et al., 2010) to generate RFP-ATG8i fusion. The DNA fragment containing RFP-ATG8i fusion was amplified using the folowing primer pair: RFP-attB1-F 5'-GGG GAC AAG TTT GTA CAA AAA AGC AGG CTT TAT GGC CTC CTC CGA GGA CGT CAT C and ATG8i-attB2R-R 5'-TCA ACC AAA GGT TTT CTC ACT GGG GGA CAG CTT TCT TGT ACA AAG TGG, colned into pDONR221 (Invitrogen). The promoter region of *ATG8i*,

258 which include a 567 bp upstream region from the start codon, were amplified using the
259 following primer pair: ATG8iPro-attB4-F 5'-GGG GAC AAC TTT GTA TAG AAA AGT
260 TGC GAT AAT CAT CTT ATG TAT TGA GCT G; ATG8iPro-attB1R-R 5'-GGG GAC
261 TGC TTT TTT GTA CAA ACT TGC TTC TTC GAC CGC CCG GAG ATT TC, cloned into
262 pDONR P4-P1R. To generate RFP-ATG8e expressing plants under the control of ATG8i
263 promoter, pDONR221 containing *RFP-ATG8i* fusion was transferred into R4pGWB501
264 destination vector with pDONR P4-P1R containing promoter region of *ATG8i*. The resulting
265 vectors were transformed into Col plants by Agrobacterium tumefaciens through the floral dip
266 method (Clough and Bent, 1998). Genotypic analysis of the segregating populations was then
267 performed in the T2 generation and each T3 homozygote line was used for the expression
268 analysis.
269 Seeds were sterilized for 12 min in 5% (v/v) sodium hypochlorite containing 0.05% (v/v)
270 Tween 20, washed with distilled water, and sown on 0.8% (w/v) Agar (Wako) containing 1/2
271 MS medium (Sigma-Aldrich), and 2% (w/v) sucrose in a plastic plate (ø 60 mm). Upon
272 germination, plates were set in a vertical position so that the seedlings grew straight along the
273 surface of the medium. The seedlings were then grown at 23 °C in a growth chamber (Sanyo)
274 with a 16-h light/8-h dark cycle under fluorescent light (100 μmol photons m^{-2} s^{-1}). Seedlings
275 with straight roots, 1.0–1.5 cm in length, were used for the experiments of gene expression
276 and retardation of seedling root growth by elevated temperatures.
277 Ten-day-old seedlings were transplanted into soil (1:1 mixture of Supermix A [Sakata]
278 and vermiculite [Nittai]) and grown as above. At initial anthesis, 3-week-old plants were
279 transferred to 30 °C and grown for 30 days as HT treatment. To study the effects of elevated
280 temperature on reproductive development, we monitored the primary inflorescence. As a male
281 sterility test, the pollination of WT and *atg* plants transferred to 30 °C for 7 days were
282 performed with WT and *atg* pollen raised at either 23 or 30 °C.
283

284 **Cytological analysis**

285 For transmission electron microscopy, dissected anthers were fixed in 2% paraformaldehyde
286 and 2% glutaraldehyde in 0.05 M cacodylate buffer (pH 7.4) at 4 °C for 24 h. They were then
287 washed 3 times in 0.05 M cacodylate buffer for 30 min each, post-fixed in 2% osmium
288 tetroxide at 4 °C for 4 h, dehydrated through a 70% to 100% alcohol series for 30 min each,
289 rinsed twice for 1 h in propylene oxide, and embedded in resin (Quetol 651; Nisshin EM Co.)
290 for 48 h at 60 °C. Ultra-thin sections (80 nm) were mounted onto copper grids with a diamond

knife on an ultramicrotome (Ultracut UCT, Leica), stained with 2% uranyl acetate at room temperature for 15 min and secondary-stained with Lead stain solution (Sigma-Aldrich) at room temperature for 3 min, and examined by transmission electron microscopy (JEM-1400 Plus, 80 kV; JEOL).

The YFP-ATG8e, and RFP-AtATG8i fluorescent signals in developing anthers and seedling roots were observed with a confocal laser scanning microscope (FV-10, Olympus) and a fluorescence microscope (BX51, Olympus), respectively, with visualization under constant excitation and the same exposure period for fluorescence. YFP and RFP fluorescent images were respectively visualized by Green and Red color.

qRT-PCR analysis

Total RNA was isolated from Arabidopsis anthers (30 to 50 stamens) and seedling roots (5 to 10 roots) in Trizol Reagent (Invitrogen). Real-time quantitative RT-PCR was performed with a PrimeScript II 1st strand cDNA Synthesis Kit (TaKaRa Bio) and SYBR Premix Ex Taq II (TaKaRa Bio), in a CFX96 Real-Time System (Bio-Rad Laboratories), with the following forward and reverse primers: 5′-GGA GAA GGC TGG ACA AAG TGA TGT-3′ and 5′-TAG ATC GCA GAC ATC AAT GCA GCA-3′ for *ATG8a*, 5′-TCA AGC GTT TAC GAG GAT AAG AAA-3′ and 5′-TGT TCT CGC CAC TGT AAG TGA TG-3′ for *ATG8e*, 5′-TGT CAA CAA CAC TCT CCC TCA-3′ and 5′-AAC CAA AGG TTT TCT CAC TGC-3′ for *ATG8i,* 5′-TGT CAA TCC TGA TGA GGC TGT T-3′ and 5′-TCA CCG CGG AGG ATA CCA-3′ for *HSP70,* 5′-CGA GAA ATC GGG AGA ATT AGC TT-3′ and 5′-GTG TTG CGA TTA ACC ACT TTT TTG-3′ for *HSP17.4*, and 5′-CCA GCT TTG GTG ATT TGA AC-3′ and 5′-CAA GCT TTC GGA GGT CAG AG-3′ for *Tubulin 2/3*.

Statistical analysis

Each series of experiments was performed in triplicate. Statistics were calculated in MS Excel software. Statistical significance was assessed by an unpaired Student's two-tailed *t*-test. Values were considered statistically significant at $P < 0.05$ and $P < 0.01$.

Acknowledgements

We thank Dr. H. Ishida, Tohoku University (Sendai, Japan), Dr. K. Yoshimoto, Meiji University (Tokyo, Japan), and the Nottingham Arabidopsis Resource Centre (Nottingham, UK) for kindly supplying the *atg* mutants and GFP recombinant lines; and Dr. H. Ishida and Dr. K. Kuchitsu, Tokyo University of Science (Chiba, Japan) for helpful suggestions. This

work was funded in part by Ministry of Education, Culture, Sports, Science and Technology grants 15H04616 and 26506001.

Author contributions

AH designed and performed the experiments, analyzed the data, prepared all figures, and wrote the manuscript; ZS, MK, SN, and MI designed and performed experiments. All authors approved the manuscript.

Conflict of interest

The authors declare that they have no conflict of interest.

Figure legends

Figure 1. An elevated temperature of 30 °C causes complete sterility in *atg* mutants. Numbers indicate flowering position. (A) Typical primary inflorescence of plants grown at 23 °C just before transfer to 30 °C. (B–F) At 23 °C (blue), silique length was unaffected. At 30 °C (orange), silique length was drastically reduced from the 5th flower in (B) WT, (C) *atg2-1*, (D) *atg5-1*, (E) *atg7-2*, and (F) *atg10-1* plants. Values are means ± SD, $n = 6$.

Figure 2. HT at 30 °C causes sporophytic male sterility in the *atg* mutant. Phenotypes of siliques of (A, B) WT Col-0, (C, D) *atg2-1*, (E) *atg5-1*, (F) *atg7-2*, and (G) *atg10-1* plants grown at 23 °C for 4 weeks (blue: A, C) or at 30 °C for 3 to 4 weeks (orange: B, D–G) arranged in developmental order from the last flowering. (H) WT Col-0 flowers of 4-week-old plants grown at 30 °C for one week were pollinated with their own pollen (left: "self") or with Col-0 pollen grown at 23 °C (right: "+♂") and following cultured for one week at 30 °C. (I) *atg5-1* flowers of 4-week-old plants grown at 30 °C for one week were pollinated with their own pollen (left: "self") or with *atg5-1* pollen grown at 23 °C (right: "+♂") and following cultured for one week at 30 °C. Scale bars, 1.0 mm.

Figure 3. HT at 30 °C causes abortion of microspores but not of ovules in *atg5-1* mutant at floral stage 13. (A–D) Phenotypes of anthers and pistil, (E–H) horizontal cross-section of pistil stained with 0.05% toluidine blue, (I–L) anther stained with KI solution, and (M–P) horizontal cross-section of anther stained with 0.05% toluidine blue of (left two columns) WT Col-0 and (right two columns) *atg5-1* plants grown at (blue) 23 °C or (orange) 30 °C. Green arrowheads show normally developing megaspores. Red arrows and T show undegenerated tapetum cells in *atg5-1* mutant at 30 °C. Scale bars, 100 μm.

Figure 4. Autophagy is induced in tapetum cells and microspores by HT. Transmission

electron microscopy images of developing anther at uninucleate stage in (A–F) WT Col-0 and (G–L) *atg5-1* mutant at (blue) 23 °C or (orange) 30 °C for 3 days. UN: Uninucleate pollen; LB: lipid body; TS: tapetosome; EP: elaioplast. V: larger vacuoles, SM: aborted microspore, ST: abnormally shrunken tapetum cell, ALB: LB increasing density but not captured, VT: abnormally larger vacuoles in the tapetum in *atg5-1* mutant (Purple colored). Blue arrows: vacuoles captured cytoplasms, vacuolization of elaioplasts (EP) and tapetosomes (TS), and lipophagy-like lipid bodies trapped in their vacuoles (LB) in WT at 30 °C. Scale bars, 10 µm.

Figure 5. ATG8e and 8i reliable molecular markers of autophagy showed increased fluorescence in the developing anther at floral stage 10-11. (A–D) YFP-ATG8e and (E–H) RFP-ATG8i signals induced in developing anthers grown for 3 days. (A, C, E, G) Fluorescence and (B, D, F, H) phase contrast merged images of anthers grown at (blue) 23 °C or (orange) 30 °C. YFP and RFP fluorescent images were respectively visualized by Green and Red color under constant excitation and the same exposure period for fluorescence. Scale bar, 100 µm.

Figure 6. Upregulation of *ATG8a*, *8e*, and *8i* genes in developing (floral stage 10-11) anthers of WT Col-0 grown at 23 or 30 °C for 3 days. The expression levels were monitored using real-time quantitative PCR and normalized to expression of *Tubulin 2/3*. Values in the controls indicate the average expression level. Bars show ±SD. * $P<0.05$. ** $P<0.01$.

Figure 7. Altered expression of *MYB80*, *UNDEAD*, *VGD1*, and *GLOX1* genes in developing (floral stage 10-11) anthers of WT Col-0 grown at 23 or 30 °C for 3 days. The expression levels were monitored using real-time quantitative PCR and normalized to expression of *Tubulin 2/3*. Values in the controls indicate the average expression level. Bars show ±SD. * $P<0.05$. ** $P<0.01$.

Figure 8. YFP-ATG8e signal induced in seedling roots grown at 23 or 30 °C for 3 days by inhibitors of auxin transport and biosynthesis. YFP-ATG8e fluorescence and phase contrast merged image (mock control at 23 °C: A, B; at 30 °C: C, D). YFP-ATG8e fluorescence and phase contrast merged image with 25 µM TIBA treatment for 3 days (at 23 °C: E, F; at 30 °C: G, H). YFP-ATG8e fluorescence and phase contrast merged image with 2.5 µM kynurenine treatment for 3 days (at 23 °C: I, J; at 30 °C: K, L). YFP fluorescent image was visualized by Green color under constant excitation and the same exposure period for fluorescence. White box represents increasing fluorescence in elongation zone. Scale bar, 100 µm.

Figure 9. Upregulation of *ATG8a*, *ATG8e*, and *ATG8i* in seedling roots of wild-type Col-0 grown at (blue) 23 °C or (orange) 30 °C by inhibitors of auxin transport and biosynthesis. The expression levels were monitored using real-time quantitative PCR and normalized to

expression of *Tubulin 2/3*. +TIBA: 25 μM TIBA treatment for 3 days. +Kyn: 2.5 μM kynurenine treatment for 3 days. Values in the control indicate the average expression level. Bars show ±SD. * $P<0.05$. ** $P<0.01$.

Figure 10. Retardation of seedling root growth by elevated temperatures. (A) Three-day-old seedlings of WT Col-0 and *atg* mutant plants were grown for 4 days at (blue) 23 °C, (orange) 30 °C, or (red) 35 °C. (B) Root length. Bars show ±SD.

Figure 11. Expression of *HSP70* and *HSP17.4* genes in developing anthers and seedling roots of WT Col-0 at (blue) 23 °C, (orange) 30 °C, or (red) 35 °C. The expression levels were monitored using real-time quantitative PCR and normalized to expression of *Tubulin 2/3*. Values in the controls indicate the average expression level. Bars show ±SD. * $P<0.05$. ** $P<0.01$.

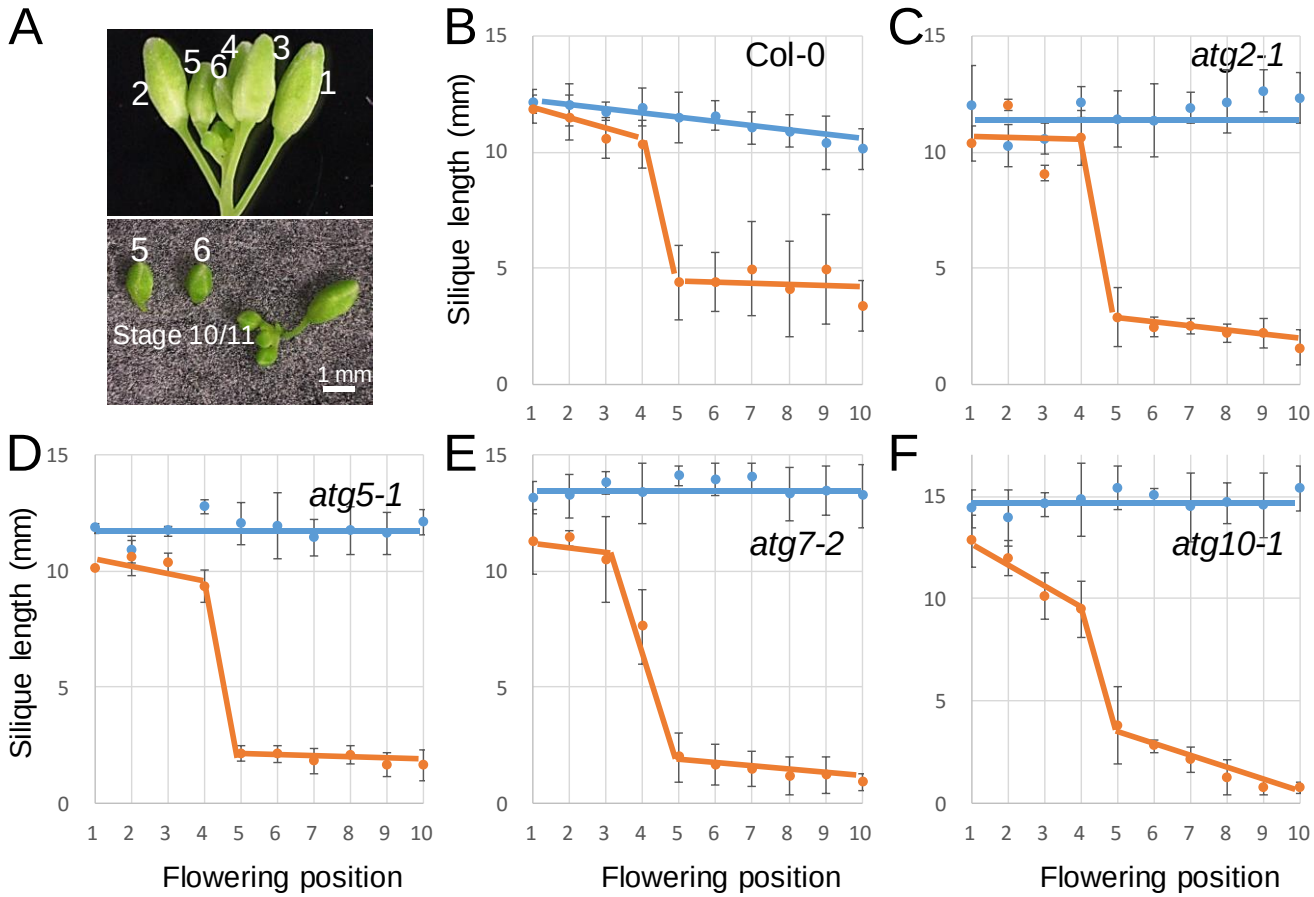

Figure 1. An elevated temperature of 30 ° C causes complete sterility in *atg* mutants. Numbers indicate flowering position. (A) Typical primary inflorescence of plants grown at 23 ° C just before transfer to 30 ° C. (B–F) At 23 ° C (blue), silique length was unaffected. At 30 ° C (orange), silique length was drastically reduced from the 5th flower in (B) WT, (C) *atg2-1*, (D) *atg5-1*, (E) *atg7-2*, and (F) *atg10-1* plants. Values are means ± SD, n = 6.

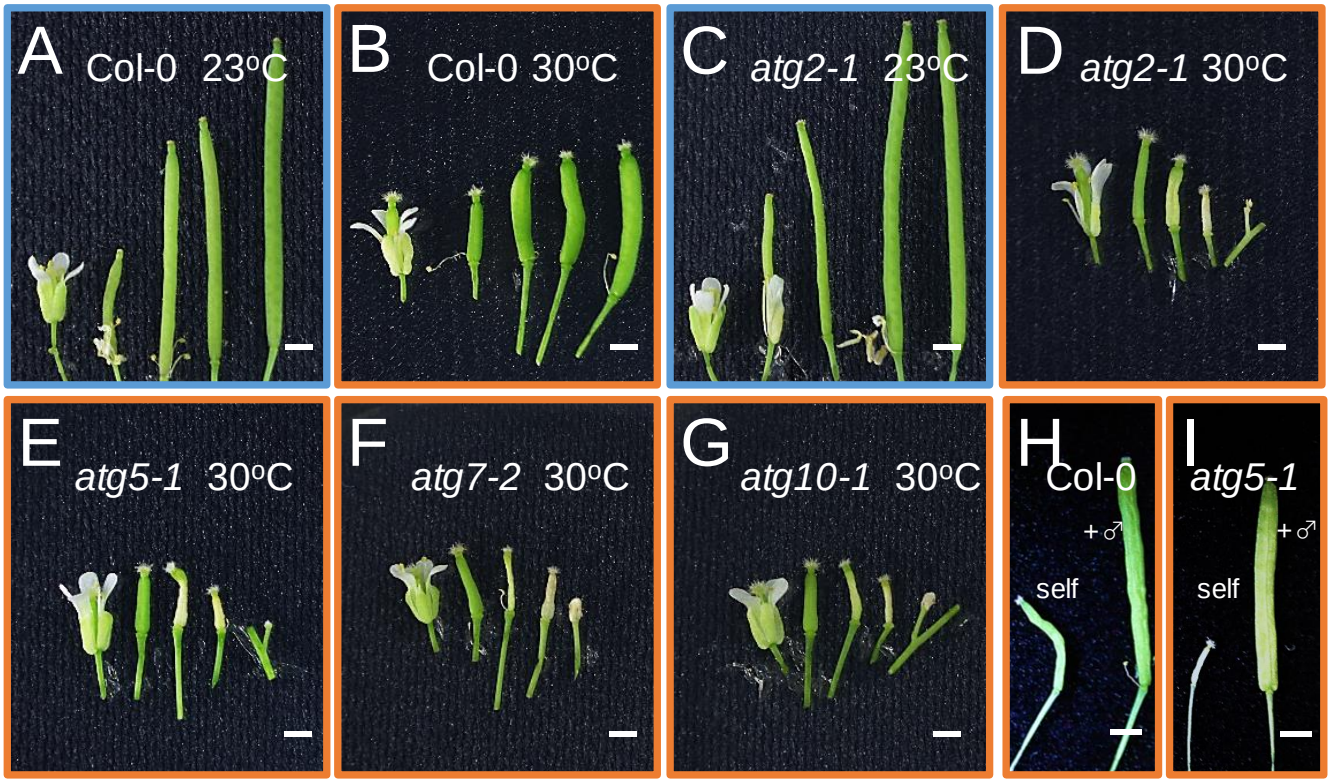

Figure 2. HT at 30 ° C causes sporophytic male sterility in the *atg* mutant.
Phenotypes of siliques of (A, B) WT Col-0, (C, D) *atg2-1*, (E) *atg5-1*, (F) *atg7-2*, and (G) *atg10-1* plants grown at 23 ° C for 4 weeks (blue: A, C) or at 30 ° C for 3 to 4 weeks (orange: B, D–G) arranged in developmental order from the last flowering. (H) WT Col-0 flowers of 4-week-old plants grown at 30 ° C for one week were pollinated with their own pollen (left: "self") or with Col-0 pollen grown at 23 ° C (right: "+♂") and following cultured for one week at 30 ° C. (I) *atg5-1* flowers of 4-week-old plants grown at 30 ° C for one week were pollinated with their own pollen (left: "self") or with *atg5-1* pollen grown at 23 ° C (right: "+♂") and following cultured for one week at 30 ° C. Scale bars, 1.0 mm.

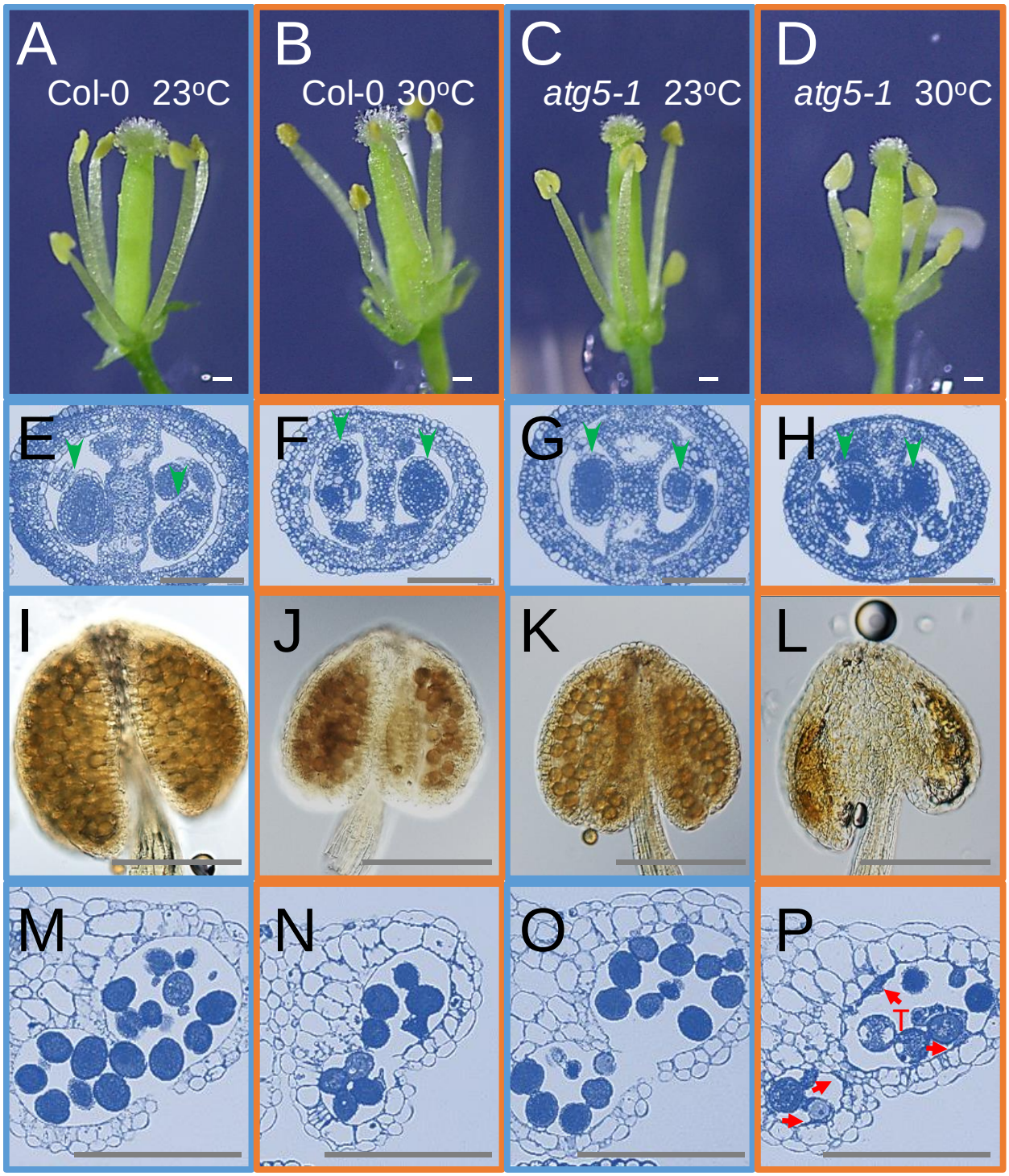

Figure 3. HT at 30 ° C causes abortion of microspores but not of ovules in *atg5-1* mutant at floral stage 13. (A–D) Phenotypes of anthers and pistil, (E–H) horizontal cross-section of pistil stained with 0.05% toluidine blue, (I–L) anther stained with KI solution, and (M–P) horizontal cross-section of anther stained with 0.05% toluidine blue of (left two columns) WT Col-0 and (right two columns) atg5-1 plants grown at (blue) 23 ° C or (orange) 30 ° C. Green arrowheads show normally developing megaspores. Red arrows and T show undegenerated tapetum cells in *atg5-1* mutant at 30 ° C. Scale bars, 100 µm.

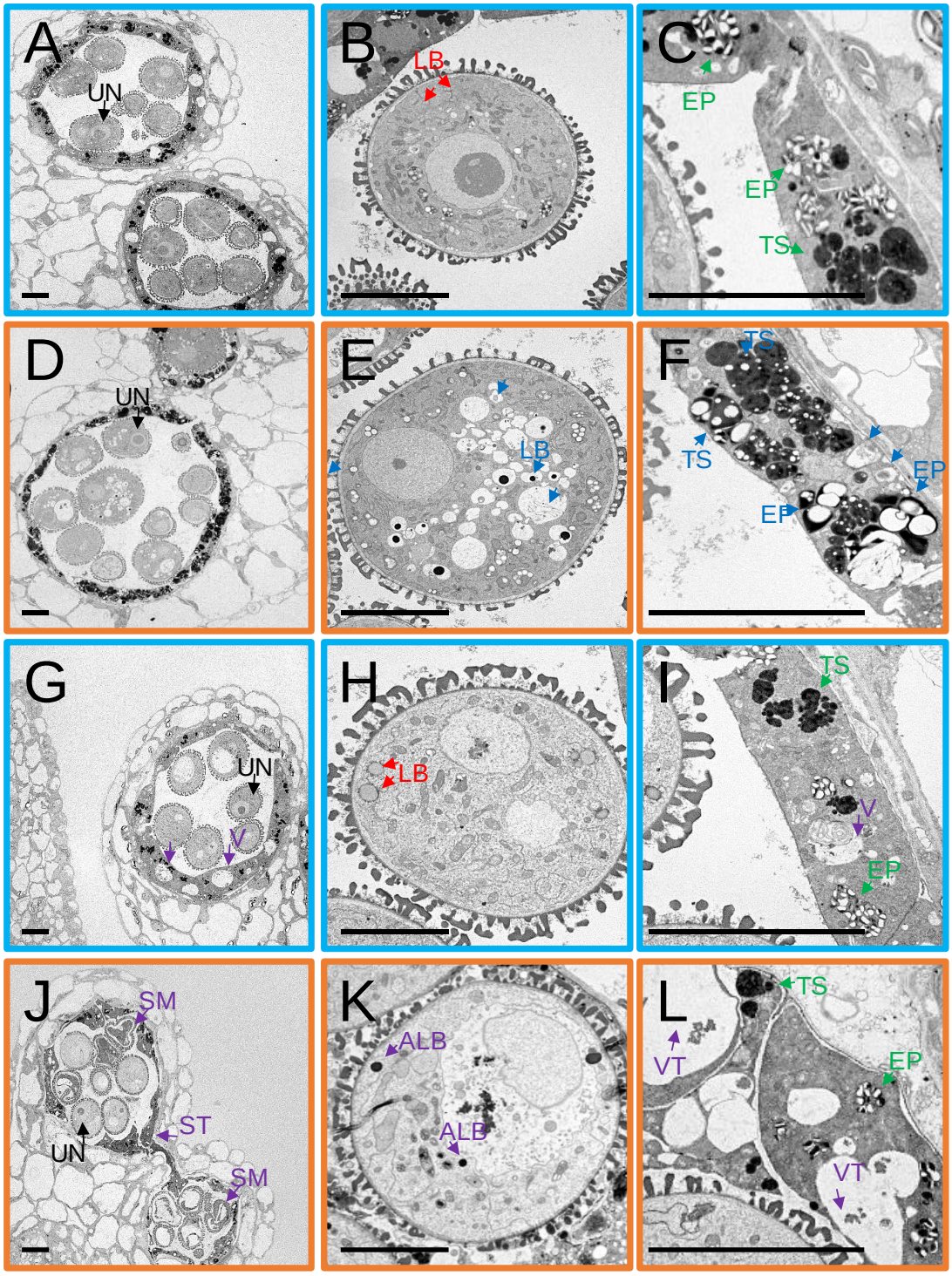

Figure 4. Autophagy is induced in tapetum cells and microspores by HT. Transmission electron microscopy images of developing anther at uninucleate stage in (A–F) WT Col-0 and (G–L) *atg5-1* mutant at (blue) 23 ° C or (orange) 30 ° C for 3 days. UN: Uninucleate pollen; LB: lipid body; TS: tapetosome; EP: elaioplast. V: larger vacuoles, SM: aborted microspore, ST: abnormally shrunken tapetum cell, ALB: LB increasing density but not captured, VT: abnormally larger vacuoles in the tapetum in *atg5-1* mutant (Purple colored). Blue arrows: vacuoles captured cytoplasms, vacuolization of elaioplasts (EP) and tapetosomes (TS), and lipophagy-like lipid bodies trapped in their vacuoles (LB) in WT at 30 ° C. Scale bars, 10 µm.

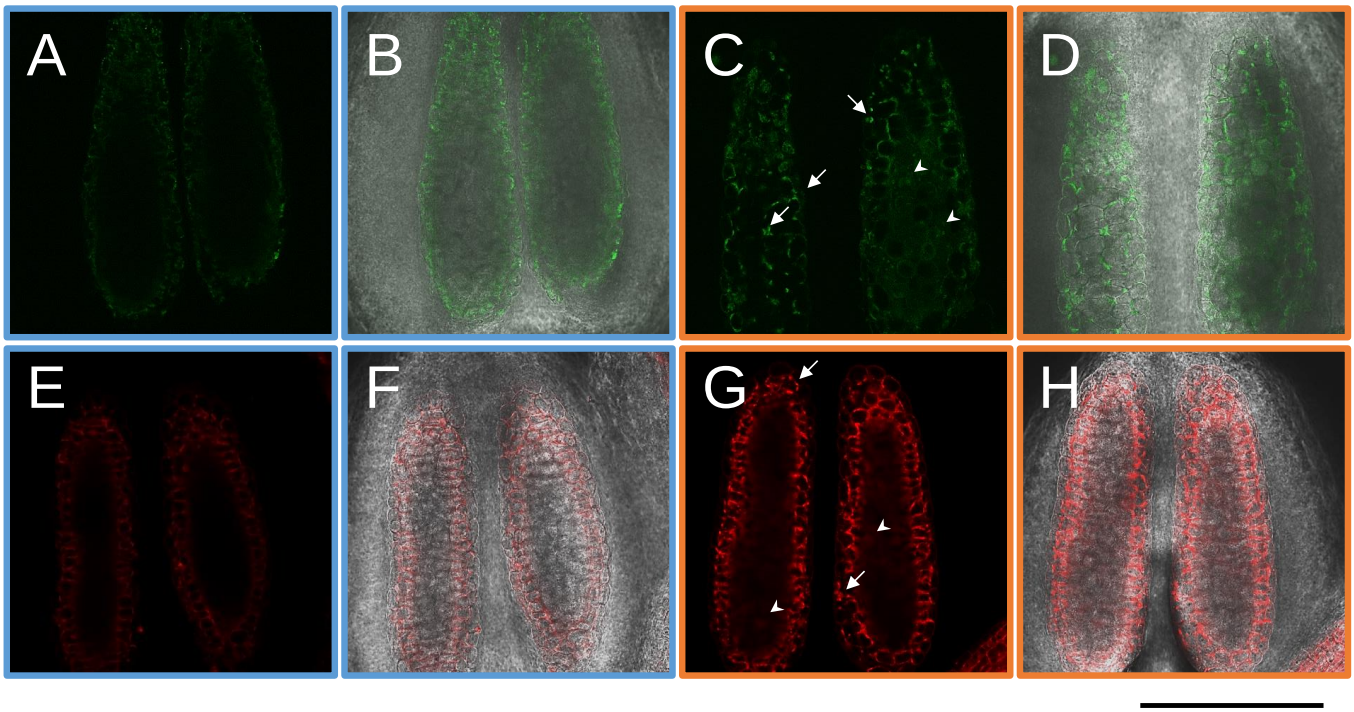

Figure 5. ATG8e and 8i reliable molecular markers of autophagy showed increased fluorescence in the developing anther at floral stage 10-11. (A–D) YFP-ATG8e and (E–H) RFP-ATG8i signals induced in developing anthers grown for 3 days. (A, C, E, G) Fluorescence and (B, D, F, H) phase contrast merged images of anthers grown at (blue) 23 ° C or (orange) 30 ° C. YFP and RFP fluorescent images were respectively visualized by Green and Red color under constant excitation and the same exposure period for fluorescence. Scale bar, 100 µm.

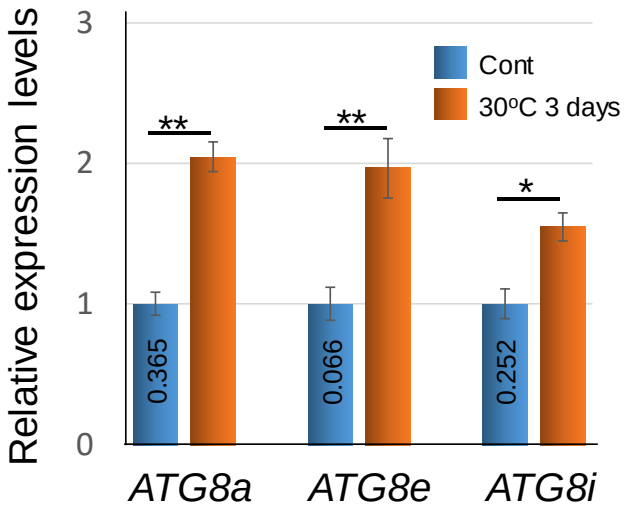

Figure 6. Upregulation of *ATG8a*, *8e*, and *8i* genes in developing (floral stage 10-11) anthers of WT Col-0 grown at 23 or 30 ° C for 3 days. The expression levels were monitored using real-time quantitative PCR and normalized to expression of *Tubulin 2/3*. Values in the controls indicate the average expression level. Bars show ±SD. * $P<0.05$. ** $P<0.01$.

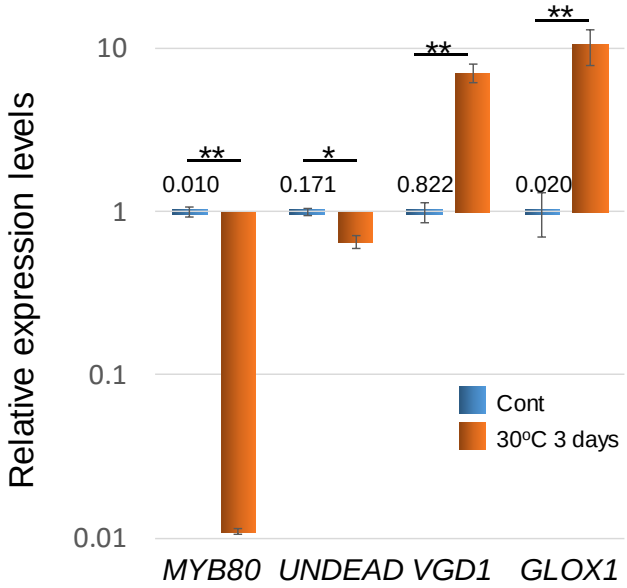

Figure 7. Altered expression of *MYB80*, *UNDEAD*, *VGD1*, and *GLOX1* genes in developing (floral stage 10-11) anthers of WT Col-0 grown at 23 or 30 ° C for 3 days. The expression levels were monitored using real-time quantitative PCR and normalized to expression of *Tubulin 2/3*. Values in the controls indicate the average expression level. Bars show ±SD. * $P<0.05$. ** $P<0.01$.

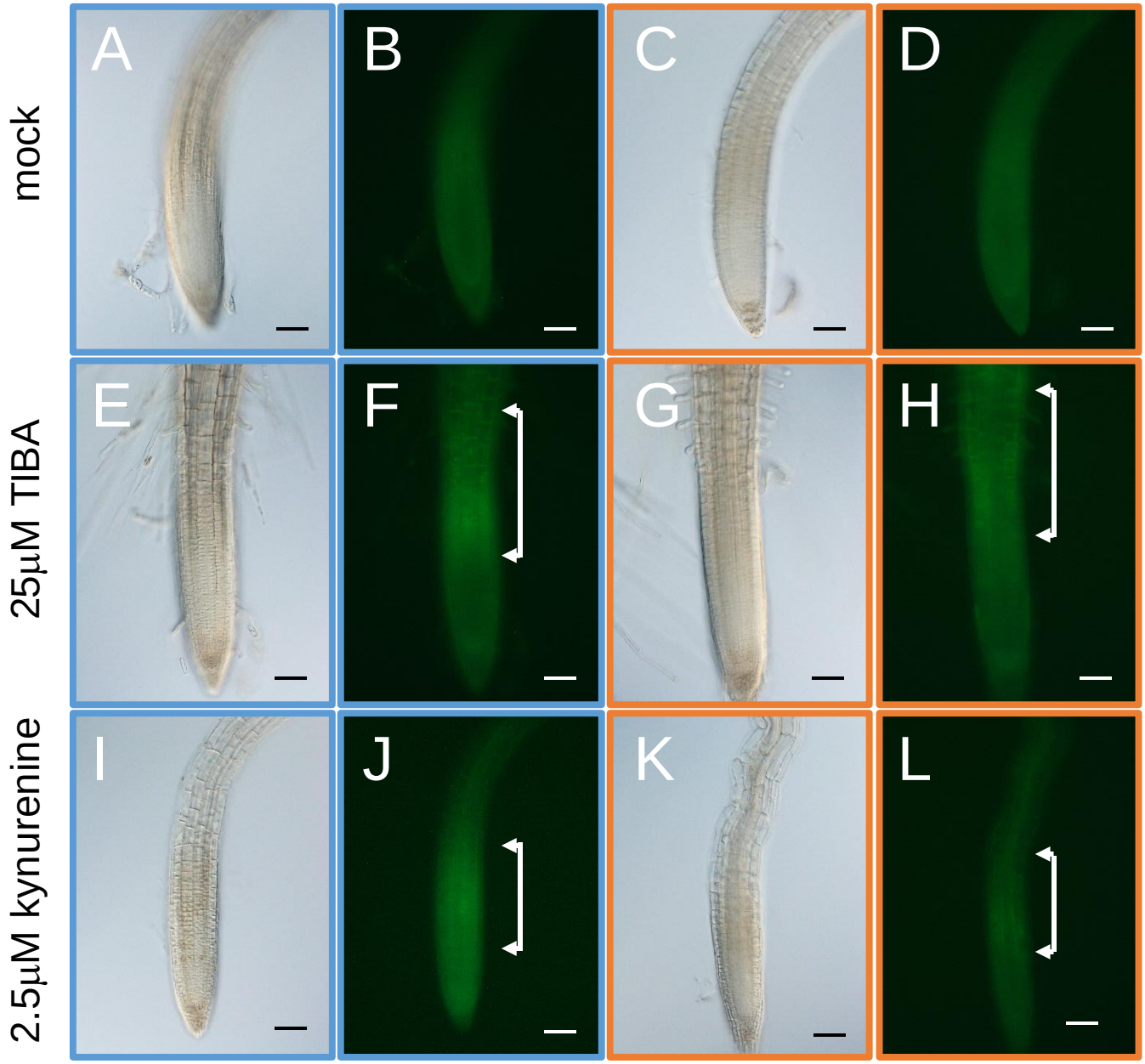

Figure 8. YFP-ATG8e signal induced in seedling roots grown at 23 or 30 ° C for 3 days by inhibitors of auxin transport and biosynthesis. YFP-ATG8e fluorescence and phase contrast merged image (mock control at 23 ° C: A, B; at 30 ° C: C, D). YFP-ATG8e fluorescence and phase contrast merged image with 25 μM TIBA treatment for 3 days (at 23 ° C: E, F; at 30 ° C: G, H). YFP-ATG8e fluorescence and phase contrast merged image with 2.5 μM kynurenine treatment for 3 days (at 23 ° C: I, J; at 30 ° C: K, L). YFP fluorescent image was visualized by Green color under constant excitation and the same exposure period for fluorescence. White box represents increasing fluorescence in elongation zone. Scale bar, 100 μm.

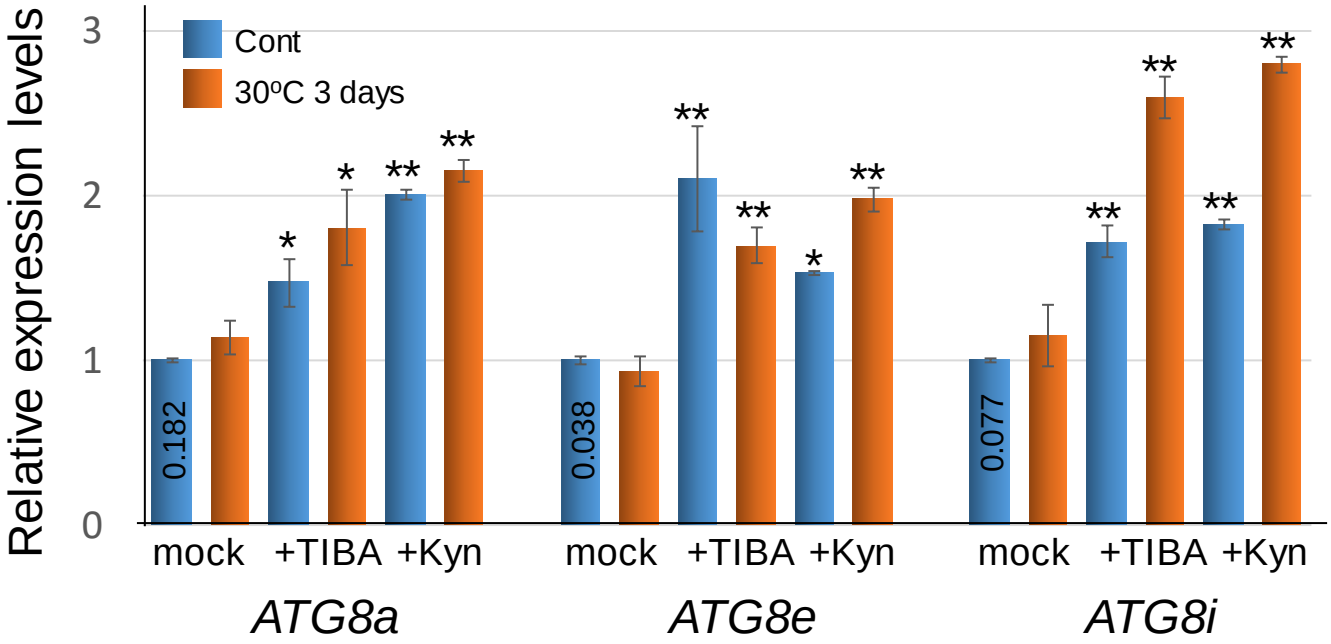

Figure 9. Upregulation of *ATG8a*, *ATG8e*, and *ATG8i* in seedling roots of wild-type Col-0 grown at (blue) 23 ° C or (orange) 30 ° C by inhibitors of auxin transport and biosynthesis. The expression levels were monitored using real-time quantitative PCR and normalized to expression of *Tubulin 2/3*. +TIBA: 25 µM TIBA treatment for 3 days. +Kyn: 2.5 µM kynurenine treatment for 3 days. Values in the control indicate the average expression level. Bars show ±SD. * $P<0.05$. ** $P<0.01$.

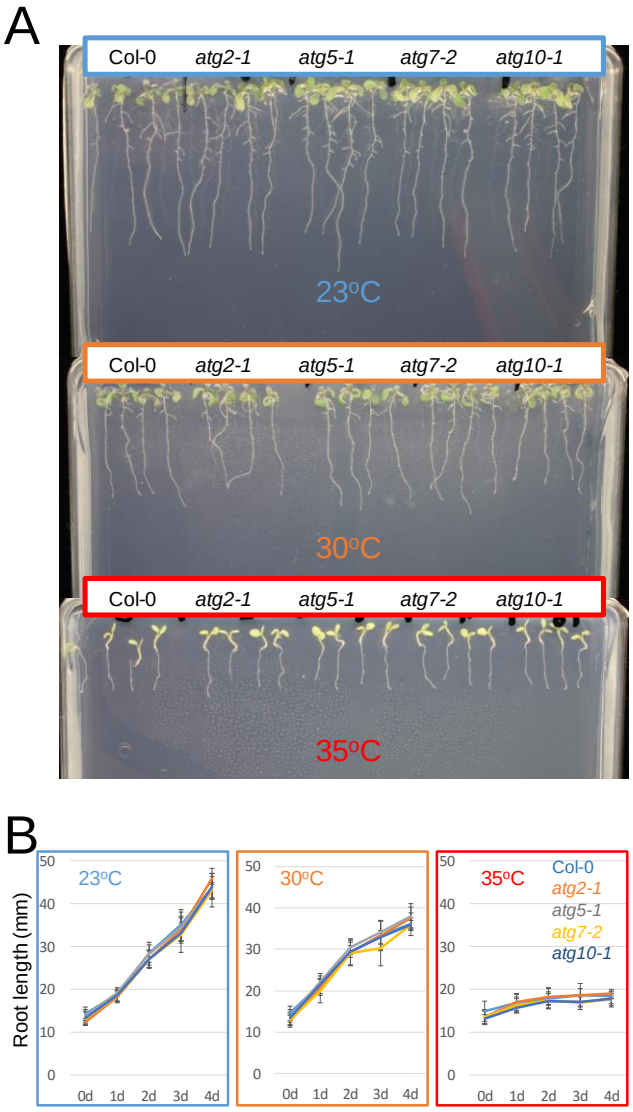

Figure 10. Retardation of seedling root growth by elevated temperatures. (A) Three-day-old seedlings of WT Col-0 and atg mutant plants were grown for 4 days at (blue) 23 ° C, (orange) 30 ° C, or (red) 35 ° C. (B) Root length. Bars show ±SD.

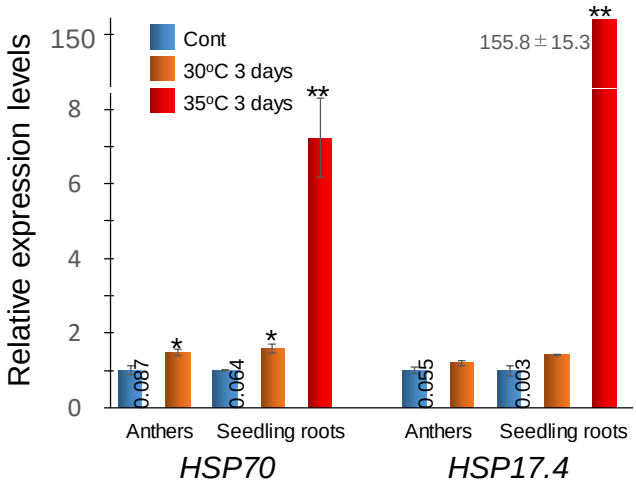

Figure 11. Expression of *HSP70* and *HSP17.4* genes in developing anthers and seedling roots of WT Col-0 at (blue) 23 ° C, (orange) 30 ° C, or (red) 35 ° C. The expression levels were monitored using real-time quantitative PCR and normalized to expression of *Tubulin 2/3*. Values in the controls indicate the average expression level. Bars show ±SD. * *P*<0.05. ***P*<0.01.

Parsed Citations

Abiko M, Akibayashi K, Sakata T, Kimura M, Kihara M, Itoh K, Asamizu E, Sato S, Takahashi H, Higashitani A. (2005) High-temperature induction of male sterility during barley (Hordeum vulgare L.) anther development is mediated by transcriptional inhibition. Sex Plant Reprod 18: 91-100. DOI: 10.1007/s00497-005-0004-2

Pubmed: Author and Title
CrossRef: Author and Title
Google Scholar: Author Only Title Only Author and Title

Baehrecke EH (2005) Autophagy: dual roles in life and death? Nat Rev Mol Cell Biol 6: 505-510. DOI: 10.1038/nrm1666

Pubmed: Author and Title
CrossRef: Author and Title
Google Scholar: Author Only Title Only Author and Title

Bassham DC, Laporte M, Marty F, Moriyasu Y, Ohsumi Y, Olsen LJ, Yoshimoto K. (2006) Autophagy in development and stress responses of plants. Autophagy 2: 2-11. DOI: 10.4161/auto.2092

Pubmed: Author and Title
CrossRef: Author and Title
Google Scholar: Author Only Title Only Author and Title

Chung T, Suttangkakul A, Vierstra RD. (2009) The ATG autophagic conjugation system in maize: ATG transcripts and abundance of the ATG8-lipid adduct are regulated by development and nutrient availability. Plant Physiol 149: 220-234. DOI: 10.1104/pp.108.126714

Pubmed: Author and Title
CrossRef: Author and Title
Google Scholar: Author Only Title Only Author and Title

Dhonukshe P, Grigoriev I, Fischer R, Tominaga M, Robinson DG, Hasek J, Paciorek T, Petrásek J, Seifertová D, Tejos R, Meisel LA, Zazímalová E, Gadella TW Jr, Stierhof YD, Ueda T, Oiwa K, Akhmanova A, Brock R, Spang A, Friml J. (2008) Auxin transport inhibitors impair vesicle motility and actin cytoskeleton dynamics in diverse eukaryotes. Proc Natl Acad Sci U S A 105: 4489-4494. DOI: 10.1073/pnas.0711414105.

Pubmed: Author and Title
CrossRef: Author and Title
Google Scholar: Author Only Title Only Author and Title

Doelling JH, Walker JM, Friedman EM, Thompson AR, Vierstra RD. (2002) The APG8/12-activating enzyme APG7 is required for proper nutrient recycling and senescence in Arabidopsis thaliana. J Biol Chem 277: 33105-33114. DOI: 10.1074/jbc.M204630200

Pubmed: Author and Title
CrossRef: Author and Title
Google Scholar: Author Only Title Only Author and Title

Dong H, Czaja M J. (2011) Regulation of lipid droplets by autophagy [J]. Trends Endocr Metab 22: 234-240. DOI: 10.1016/j.tem.2011.02.003

Pubmed: Author and Title
CrossRef: Author and Title
Google Scholar: Author Only Title Only Author and Title

Grefen C, Donald N, Hashimoto K, Kudla J, Schumacher K, Blatt MR. (2010) A ubiquitin-10 promoter-based vector set for fluorescent protein tagging facilitates temporal stability and native protein distribution in transient and stable expression studies. Plant J 64: 355-365. DOI: 10.1111/j.1365-313X.2010.04322.x.

Pubmed: Author and Title
CrossRef: Author and Title
Google Scholar: Author Only Title Only Author and Title

Hanamata S, Kurusu T, Kuchitsu K. (2014) Roles of autophagy in male reproductive development in plants. Front Plant Sci 5: 457. DOI: 10.3389/fpls.2014.00457.

Pubmed: Author and Title
CrossRef: Author and Title
Google Scholar: Author Only Title Only Author and Title

Hanaoka H, Noda T, Shirano Y, Kato T, Hayashi H, Shibata D, Tabata S, Ohsumi Y. (2002) Leaf senescence and starvation-induced chlorosis are accelerated by the disruption of an Arabidopsis autophagy gene. Plant Physiol 129: 1181-1193. DOI: 10.1104/pp.011024

Pubmed: Author and Title
CrossRef: Author and Title
Google Scholar: Author Only Title Only Author and Title

He W, Brumos J, Li H, Ji Y, Ke M, Gong X, Zeng Q, Li W, Zhang X, An F, Wen X, Li P, Chu J, Sun X, Yan C, Yan N, Xie DY, Raikhel N, Yang Z, Stepanova AN, Alonso JM, Guo H. (2011) A small-molecule screen identifies l-kynurenine as a competitive inhibitor of TAA1/TAR activity in ethylene-directed auxin biosynthesis and root growth in Arabidopsis. Plant Cell 23: 3944-3960. DOI: 10.1105/tpc.111.089029.

Pubmed: Author and Title
CrossRef: Author and Title
Google Scholar: Author Only Title Only Author and Title

Hofius D, Munch D, Bressendorff S, Mundy J, Petersen M. (2011) Role of autophagy in disease resistance and hypersensitive response-associated cell death. Cell Death Differ 18: 1257-1262. DOI: 10.1038/cdd.2011.43.

Pubmed: Author and Title
CrossRef: Author and Title
Google Scholar: Author Only Title Only Author and Title

Ishida H, Yoshimoto K, Izumi M, Reisen D, Yano Y, Makino A, Ohsumi Y, Hanson MR., Mae T. (2008) Mobilization of rubisco and stromatolites localized fluorescent proteins of chloroplasts to the vacuole by an ATG gene-dependent autophagic process. Plant Physiol 148: 142-155. DOI: 10.1104/pp.108.122770
Pubmed: Author and Title
CrossRef: Author and Title
Google Scholar: Author Only Title Only Author and Title

Kim I, Rodriguez-Enriquez S, Lemasters JJ (2007) Selective degradation of mitochondria by mitophagy. Arch Biochem Biophys 462: 245-253. DOI: 10.1016/j.abb.2007.03.034
Pubmed: Author and Title
CrossRef: Author and Title
Google Scholar: Author Only Title Only Author and Title

Klionsky DJ, Emr SD (2000) Autophagy as a regulated pathway of cellular degradation. Science 290: 1717-1721. DOI: 10.1126/science.290.5497.1717
Pubmed: Author and Title
CrossRef: Author and Title
Google Scholar: Author Only Title Only Author and Title

Kroemer G, Jäättelä M (2005) Lysosomes and autophagy in cell death control. Nat Rev Cancer 5: 886-897. DOI: 10.1038/nrc1738
Pubmed: Author and Title
CrossRef: Author and Title
Google Scholar: Author Only Title Only Author and Title

Kurusu T, Koyano T, Hanamata S, Kubo T, Noguchi Y, Yagi C, Nagata N, Yamamoto T, Ohnishi T, Okazaki Y, Kitahata N, Ando D, Ishikawa M, Wada S, Miyao A, Hirochika H, Shimada H, Makino A, Saito K, Ishida H, Kinoshita T, Kurata N, Kuchitsu K. (2014) OsATG7 is required for autophagy-dependent lipid metabolism in rice postmeiotic anther development. Autophagy 10: 878-888. DOI: 10.4161/auto.28279.
Pubmed: Author and Title
CrossRef: Author and Title
Google Scholar: Author Only Title Only Author and Title

Li SF, Iacuone S, Parish RW. (2007) Suppression and restoration of male fertility using a transcription factor. Plant Biotechnol J 5: 297-312. DOI: 10.1111/j.1467-7652.2007.00242.x
Pubmed: Author and Title
CrossRef: Author and Title
Google Scholar: Author Only Title Only Author and Title

Love AJ, Milner JJ, Sadanandom A. (2008) Timing is everything: regulatory overlap in plant cell death. Trends in Plant Science 13: 589-595. DOI: 10.1016/j.tplants.2008.08.006
Pubmed: Author and Title
CrossRef: Author and Title
Google Scholar: Author Only Title Only Author and Title

Merkulova EA, Guiboileau A, Naya L, Masclaux-Daubresse C, Yoshimoto K. (2014) Assessment and optimization of autophagy monitoring methods in Arabidopsis roots indicate direct fusion of autophagosomes with vacuoles. Plant Cell Physiol 55: 715-726. DOI: 10.1093/pcp/pcu041
Pubmed: Author and Title
CrossRef: Author and Title
Google Scholar: Author Only Title Only Author and Title

Mizushima N (2007) Autophagy: process and function. Genes Dev 21: 2861-2873. DOI: 10.1101/gad.1599207
Pubmed: Author and Title
CrossRef: Author and Title
Google Scholar: Author Only Title Only Author and Title

Mizushima N, Yamamoto A, Matsui M, Yoshimori T, Ohsumi Y (2004) In vivo analysis of autophagy in response to nutrient starvation using transgenic mice expressing a fluorescent autophagosome marker. Mol Biol Cell 15: 1101-1111. DOI: 10.1091/mbc.E03-09-0704
Pubmed: Author and Title
CrossRef: Author and Title
Google Scholar: Author Only Title Only Author and Title

Müller F, Rieu I. (2016) Acclimation to high temperature during pollen development. Plant Reprod 29: 107-118. DOI: 10.1007/s00497-016-0282-X.
Pubmed: Author and Title
CrossRef: Author and Title
Google Scholar: Author Only Title Only Author and Title

Nakagawa T, Nakamura S, Tanaka K, Kawamukai M, Suzuki T, Nakamura K, Kimura T, Ishiguro S. (2008) Development of R4 gateway binary vectors (R4pGWB) enabling high-throughput promoter swapping for plant research. Biosci Biotechnol Biochem 72: 624-629. DOI: 10.1271/bbb.70678
Pubmed: Author and Title
CrossRef: Author and Title
Google Scholar: Author Only Title Only Author and Title

Nakatogawa H, Suzuki K, Kamada Y, Ohsumi Y (2009) Dynamics and diversity in autophagy mechanisms: lessons from yeast. Nat Rev Mol Cell Biol. 10: 458-467. DOI: 10.1038/nrm2708.
Pubmed: Author and Title
CrossRef: Author and Title

Google Scholar: Author Only Title Only Author and Title

Nakayama M, Kaneko Y, Miyazawa Y, Fujii N, Higashitani N, Wada S, Ishida H, Yoshimoto K, Shirasu K, Yamada K, Nishimura M, Takahashi H. (2012) A possible involvement of autophagy in amyloplast degradation in columella cells during hydrotropic response of Arabidopsis roots[J]. Planta 236: 999-1012. DOI: 10.1007/s00425-012-1655-5

Pubmed: Author and Title
CrossRef: Author and Title
Google Scholar: Author Only Title Only Author and Title

Ohsumi Y (1999) Molecular mechanism of autophagy in yeast, Saccharomyces cerevisiae. Philos Trans R Soc Lond B Biol Sci 354: 1577-1581. DOI: 10.1098/rstb.1999.0501

Pubmed: Author and Title
CrossRef: Author and Title
Google Scholar: Author Only Title Only Author and Title

Oshino T, Abiko M, Saito R, Ichiishi E, Endo M, Kawagishi-Kobayashi M, Higashitani A. (2007) Premature progression of anther early developmental programs accompanied by comprehensive alterations in transcription during high-temperature injury in barley plants. Mol Genet Genom 278: 31-42. DOI: 10.1007/s00438-007-0229-x

Pubmed: Author and Title
CrossRef: Author and Title
Google Scholar: Author Only Title Only Author and Title

Oshino T, Miura S, Kikuchi S, Hamada K, Yano K, Watanabe M, Higashitani A. (2011) Auxin depletion in barley plants under high-temperature conditions represses DNA proliferation in organelles and nuclei via transcriptional alterations. Plant Cell Environ 34: 284-290. DOI: 10.1111/j.1365-3040.2010.02242.x

Pubmed: Author and Title
CrossRef: Author and Title
Google Scholar: Author Only Title Only Author and Title

Papini A, Mosti S, Brighigna L. (1999) Programmed-cell-death events during tapetum development of angiosperms. Protoplasma 207: 213-221. DOI: 10.1007/BF01283002

Pubmed: Author and Title
CrossRef: Author and Title
Google Scholar: Author Only Title Only Author and Title

Parish RW, Li SF. (2010) Death of a tapetum: A programme of developmental altruism. Plant Science 178:73-89. DOI: 10.1016/j.plantsci.2009.11.001

Pubmed: Author and Title
CrossRef: Author and Title
Google Scholar: Author Only Title Only Author and Title

Phan HA, Iacuone S, Li SF, Parish RW. (2011) The MYB80 transcription factor is required for pollen development and the regulation of tapetal programmed cell death in Arabidopsis thaliana. Plant Cell 23: 2209-2224. DOI: 10.1105/tpc.110.082651

Pubmed: Author and Title
CrossRef: Author and Title
Google Scholar: Author Only Title Only Author and Title

Phan HA, Li SF, Parish RW. (2012) MYB80, a regulator of tapetal and pollen development, is functionally conserved in crops. Plant Mol Biol 78: 171-183. DOI: 10.1007/s11103-011-9855-0

Pubmed: Author and Title
CrossRef: Author and Title
Google Scholar: Author Only Title Only Author and Title

Sakata T, Higashitani A. (2008) Male sterility accompanied with abnormal anther development in plants - Genes and environmental stresses with special reference to high temperature injury. Intl J Plant Dev Biol 2: 42-51.

Pubmed: Author and Title
CrossRef: Author and Title
Google Scholar: Author Only Title Only Author and Title

Sakata T, Oshino T, Miura S, Tomabechi M, Tsunaga Y, Higashitani N, Miyazawa Y, Takahashi H, Watanabe M, Higashitani A. (2010) Auxins reverse plant male sterility caused by high temperatures. Proc Natl Acad Sci U S A 107: 8569-8574. DOI: 10.1073/pnas.1000869107.

Pubmed: Author and Title
CrossRef: Author and Title
Google Scholar: Author Only Title Only Author and Title

Singh SP, Pandey T, Srivastava R, Verma PC, Singh PK, Tuli R, Sawant SV. (2010) BECLIN1 from Arabidopsis thaliana under the generic control of regulated expression systems, a strategy for developing male sterile plants. Plant Biotechnol J 8: 1005-1022. DOI: 10.1111/j.1467-7652.2010.00527.x

Pubmed: Author and Title
CrossRef: Author and Title
Google Scholar: Author Only Title Only Author and Title

Singh SP, Singh SP, Pandey T, Singh RR, Sawant SV. (2015) A novel male sterility-fertility restoration system in plants for hybrid seed production. Scientific Rep 5: 11274. DOI: 10.1038/srep11274

Pubmed: Author and Title
CrossRef: Author and Title
Google Scholar: Author Only Title Only Author and Title

Smyth DR, Bowman JL, Meyerowitz EM. (1990) Early flower development in Arabidopsis. Plant Cell 2: 755-767. DOI:

10.1105/tpc.2.8.755
Pubmed: Author and Title
CrossRef: Author and Title
Google Scholar: Author Only Title Only Author and Title

Suzuki T, Tsunekawa S, Koizuka C, Yamamoto K, Imamura J, Nakamura K, Ishiguro S. (2013) Development and disintegration of tapetum-specific lipid-accumulating organelles, elaioplasts and tapetosomes, in Arabidopsis thaliana and Brassica napus. Plant Sci 207: 25-36. DOI: 10.1016/j.plantsci.2013.02.008.
Pubmed: Author and Title
CrossRef: Author and Title
Google Scholar: Author Only Title Only Author and Title

Varnier AL, Mazeyrat-Gourbeyre F, Sangwan RS, Clement C (2005) Programmed cell death progressively models the development of anther sporophytic tissues from the tapetum and is triggered in pollen grains during maturation. J Struct Biol 152:118-128. DOI: 10.1016/j.jsb.2005.07.011
Pubmed: Author and Title
CrossRef: Author and Title
Google Scholar: Author Only Title Only Author and Title

Wada S, Hayashida Y, Izumi M, Kurusu T, Hanamata S, Kanno K, Kojima S, Yamaya T, Kuchitsu K, Makino A, Ishida H. (2015) Autophagy supports biomass production and nitrogen use efficiency at the vegetative stage in rice. Plant Physiol 168: 60-73. DOI: 10.1104/pp.15.00242.
Pubmed: Author and Title
CrossRef: Author and Title
Google Scholar: Author Only Title Only Author and Title

Wu SS, Platt KA, Ratnayake C, Wang TW, Ting JT, Huang AH. (1997) Isolation and characterization of neutral-lipid-containing organelles and globuli-filled plastids from Brassica napus tapetum. Proc Natl Acad Sci U S A 94: 12711-12716. DOI: 10.1073/pnas.94.23.12711
Pubmed: Author and Title
CrossRef: Author and Title
Google Scholar: Author Only Title Only Author and Title

Xia K, Liu T, Ouyang J, Wang R, Fan T, Zhang M. (2011) Genome-wide identification, classification, and expression analysis of autophagy-associated gene homologues in rice (Oryza sativa L.). DNA Res 18: 363-377. DOI: 10.1093/dnares/dsr024
Pubmed: Author and Title
CrossRef: Author and Title
Google Scholar: Author Only Title Only Author and Title

Xie Z, Nair U, Klionsky DJ. (2008) Atg8 controls phagophore expansion during autophagosome formation. Mol Biol Cell 19: 3290-3298. DOI: 10.1091/mbc.E07-12-1292
Pubmed: Author and Title
CrossRef: Author and Title
Google Scholar: Author Only Title Only Author and Title

Xu Y, Iacuone S, Li SF, Parish RW. (2014) MYB80 homologues in Arabidopsis, cotton and Brassica: regulation and functional conservation in tapetal and pollen development. BMC Plant Biol 14: 278. DOI: 10.1186/s12870-014-0278-3
Pubmed: Author and Title
CrossRef: Author and Title
Google Scholar: Author Only Title Only Author and Title

Yorimitsu T, Klionsky DJ (2005) Autophagy: Molecular machinery for self-eating. Cell Death Differ 12: 1542-1552. DOI: 10.1038/sj.cdd.4401765
Pubmed: Author and Title
CrossRef: Author and Title
Google Scholar: Author Only Title Only Author and Title

Yoshimoto K. (2012) Beginning to understand autophagy, an intracellular self-degradation system in plants. Plant Cell Physiol 53: 1355-1365. DOI: 10.1093/pcp/pcs099
Pubmed: Author and Title
CrossRef: Author and Title
Google Scholar: Author Only Title Only Author and Title

Yoshimoto K, Jikumaru Y, Kamiya Y, Kusano M, Consonni C, Panstruga R, Ohsumi Y, Sirasu K. (2009) Autophagy negatively regulates cell death by controlling NPR1-dependent salicylic acid signaling during senescence and the innate immune response in Arabidopsis. Plant Cell 21: 2914-2927 DOI: 10.1105/tpc.109.068635
Pubmed: Author and Title
CrossRef: Author and Title
Google Scholar: Author Only Title Only Author and Title

Zhou J. Wang J. Yu J-Q, Chen Z. (2014) Role and regulation of autophagy in heat stress responses of tomato plants. Front Plant Sci 5: 174. DOI: 10.3389/fpls.2014.00174
Pubmed: Author and Title
CrossRef: Author and Title
Google Scholar: Author Only Title Only Author and Title